Technical Note

# Matlab-based tool for ECG and HRV analysis

Barbara Mali [a], Sara Zulj [b], Ratko Magjarevic [b], Damijan Miklavcic [a], Tomaz Jarm [a],*

[a] University of Ljubljana, Faculty of Electrical Engineering, Department of Biomedical Engineering, Trzaska 25, SI-1000 Ljubljana, Slovenia
[b] University of Zagreb, Faculty of Electrical Engineering and Computing, Department of Electronic Systems and Information Processing, Unska 3, 1000 Zagreb, Croatia

## ABSTRACT

Delivery of electroporation pulses in electroporation-based treatments could potentially induce heart-related effects. The objective of our work was to develop a software tool for electrocardiogram (ECG) analysis to facilitate detection of such effects in pre-selected ECG- or heart rate variability (HRV) parameters.

Our software tool consists of five distinct modules for: (i) preprocessing; (ii) learning; (iii) detection and classification; (iv) selection and verification; and (v) ECG and HRV analysis. Its key features are: automated selection of ECG segments from ECG signal according to specific user-defined requirements (e.g., selection of relatively noise-free ECG segments); automated detection of prominent heartbeat features, such as Q, R and T wave peak; automated classification of individual heartbeat as normal or abnormal; displaying of heartbeat annotations; quick manual screening of analyzed ECG signal; and manual correction of annotation and classification errors.

The performance of the detection and classification module was evaluated on 19 two-hour-long ECG records from Long-Term ST database. On average, the QRS detection algorithm had high sensitivity (99.78%), high positive predictivity (99.98%) and low detection error rate (0.35%). The classification algorithm correctly classified 99.45% of all normal QRS complexes. For normal heartbeats, the positive predictivity of 99.99% and classification error rate of 0.01% were achieved.

The software tool provides for reliable and effective detection and classification of heartbeats and for calculation of ECG and HRV parameters. It will be used to clarify the issues concerning patient safety during the electroporation-based treatments used in clinical practice. Preventing the electroporation pulses from interfering with the heart is becoming increasingly important because new applications of electroporation-based treatments are being developed which are using endoscopic, percutaneous or surgical means to access internal tumors or tissues and in which the target tissue can be located in immediate vicinity to the heart.

## 1. Introduction

Electroporation is a phenomenon resulting in transient increase in the cell membrane permeability due to exposure to an electric field during delivery of short, high-voltage electric pulses, i.e., electroporation pulses [1–4]. Increased membrane permeability allows molecules with intracellular targets, which under physiological conditions cannot cross the cell membrane, to enter the cell and exert their cytotoxicity [5]. Electroporation can be either reversible or irreversible, depending on electrical conditions and tissue characteristics, and both have been used in biomedical applications [6–11]. These applications include electrochemotherapy [12–18], electrotransfer for gene therapy and DNA vaccination [19–24], transdermal drug delivery [25–29], cell electrofusion [30–34], and tissue ablation [35–39]. Electroporation is also used in biotechnology and other areas [11,40].

Some of electroporation-based treatments, like electrochemotherapy, gene electrotransfer for gene therapy and DNA vaccination and non-thermal irreversible electroporation, are being successfully introduced into clinical practice. But when electroporation pulses are applied to visceral or other internal tumors and tissues there is an increased risk of inducing heart-related effects, especially when the treatment area is in vicinity of the heart [15,38,41–48]. These heart-related effects can be detected by analyzing electrocardiogram (ECG) signals recorded before, during and after the therapy.

A software tool for reliable and effective analysis of potential side-effects of electroporation pulses on ECG or heart rate

* Corresponding author. Tel.: +386 1 47 68 820; fax: +386 1 42 64 658.
*E-mail addresses:* barbara.mali@fe.uni-lj.si (B. Mali), sara.zulj@fer.hr (S. Zulj), ratko.magjarevic@fer.hr (R. Magjarevic), damijan.miklavcic@fe.uni-lj.si (D. Miklavcic), tomaz.jarm@fe.uni-lj.si (T. Jarm).
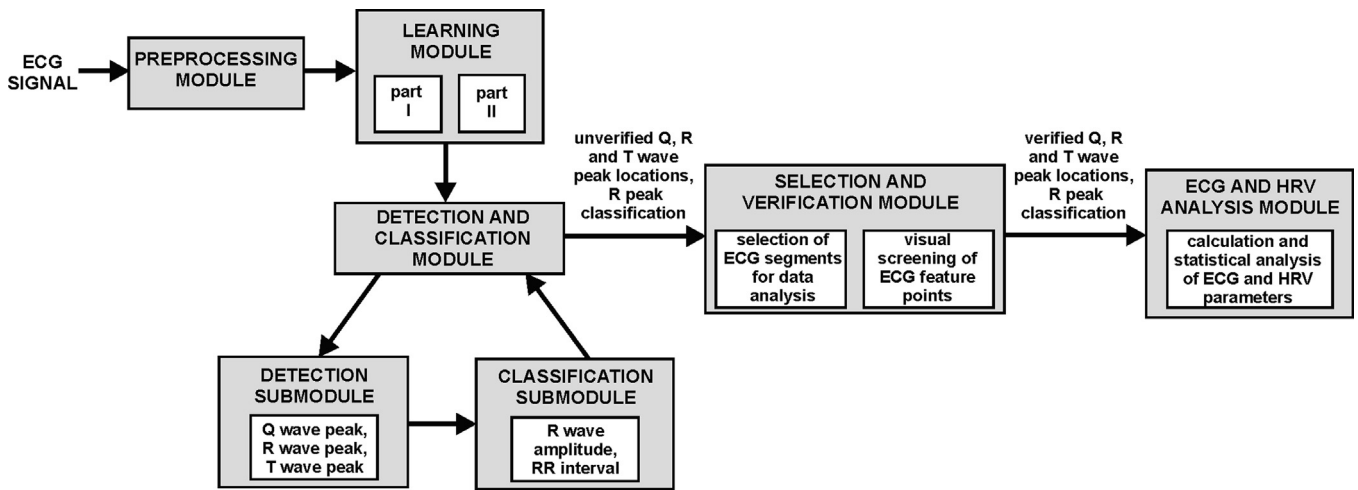
**Fig. 1.** The structure of the software tool with five main modules for: (i) preprocessing; (ii) learning; (iii) detection and classification; (iv) selection and verification; and (v) ECG and HRV analysis.

variability (HRV) parameters is therefore needed. A software tool should provide selection of ECG segments from ECG signal according to a user-defined selection criteria; detection of prominent heartbeat features, such as Q, R and T wave peaks, and classification of individual heartbeat either as normal or abnormal; and displaying, screening and possible correction of detected and classified heartbeats from analyzed ECG signal. Several software tools for HRV analysis that include calculation of various HRV parameters exist (such as Kubios, SyneScope, Biopac, Nevrokard HRV system) but none of them provides all required functionalities listed above. The objective of our study was therefore to develop a software tool that does.

## 2. Methods

### 2.1. Outline and description of the tool

Our software tool consists of five distinct modules for: (i) preprocessing; (ii) learning; (iii) detection and classification; (iv) selection and verification; and (v) ECG and HRV analysis (Fig. 1). The software tool was developed for analysis of Holter ECG signals sampled at 200 Hz. Appropriate adjustment of the implemented digital filters in the detection module would therefore be needed for signals sampled at a different frequency. Currently, the software tool accepts input ECG signals only in plain text format because we are planning to analyze the ECG signals from different origins, such as various Holter devices, Biopac system and different ECG databases. Therefore, ECG signals in other formats have to be transformed to plain text first.

### 2.1.1. Preprocessing module

The raw ECG signal is first preprocessed in sequence by band-pass filtering, differentiation, squaring, and moving-window integration, thus following the well-known Pan-Tompkins algorithm [49]. Three different signals are used for ECG analysis and serve as inputs to the learning and the detection and classification modules: the original raw ECG signal ($Y_{ECG}$), the output of the band-pass filter ($Y_{BPF}$) and the output of the moving-window integration with 30-sample window size (150 ms) ($Y_{MWI}$).

### 2.1.2. Learning module

The learning module consists of two parts. Part I is used to initialize the main threshold parameter, i.e., the threshold for QRS detection ($d_{th}$). Its value is extracted from the initial section of the preprocessed ECG signal $Y_{MWI}$ (defined in Section 2.1.1), which is derived from 16 s of noise- and arrhythmias-free ECG signal and which is divided into 1-second subintervals. Within each 1-second subinterval, the maximum value of $Y_{MWI}$ is sought for. Four largest and four smallest maximum values of $Y_{MWI}$ are discarded and the remaining eight values are averaged. This averaged value is used to initialize the $d_{th}$. In further processing of the ECG signal in detection and classification module, $d_{th}$ is updated by running averaging after each new heartbeat detected as described in Section 2.1.3.

Part II of the learning module is used to initialize values of parameters for the classification in detection and classification module; i.e., the running averages of R wave amplitude ($R_{th}$) and RR interval ($RR_{th}$). This part requires detection of 17 consecutive QRS complexes and determination of location and amplitude of 17 R wave peaks. 16 RR intervals between consecutive R wave peaks are calculated. For the details of QRS and R wave peak detection see Section 2.1.3.1. For calculation of $R_{th}$ the eight most recent values of R wave amplitude (among the 17 available) are used. Two largest and two smallest values of R wave amplitude are discarded and the remaining four values are averaged and used as the initial value of $R_{th}$. In calculation of the average RR intervals, all 16 RR interval values are considered; four largest and four smallest values are discarded and the remaining eight values are averaged and used to initialize $RR_{th}$. After the learning phase, $R_{th}$ and $RR_{th}$ are updated with every new detected heartbeat.

### 2.1.3. Detection and classification module

This module consists of the detection submodule and the classification submodule (Fig. 1). The algorithm for detection and classification of heartbeats is used to determine Q, R and T wave peak locations of individual heartbeats and to classify heartbeats as either normal or abnormal. The algorithm is based on analysis of $Y_{ECG}$, $Y_{BPF}$ and $Y_{MWI}$ signals and operates on individual signal samples in time-domain.

#### 2.1.3.1. The detection submodule.

The detection of QRS complex is based on a well-known Pan-Tompkins QRS detector [49] and supplemented with additionally extracted parameters (such as Q, R and T wave peak location, R wave amplitude, RR interval) to achieve reliable QRS detection and classification performance.

Initial detection of QRS complex is determined using adaptive threshold ($d_{QRSth}$) on $Y_{MWI}$ signal. The initial value of $d_{QRSth}$ is taken from the part I of the learning module ($d_{QRSth} = 0.125 \cdot d_{th}$). The scale factor of 0.125 was determined empirically. When the current value

of $Y_{MWI}$ exceeded $d_{QRSth}$, QRS complex was detected. The maximum value of $Y_{MWI}$ within this QRS complex was determined and included in the running average of $d_{QRSth}$, which consisted of the four most recent maximum values of $Y_{MWI}$ detected from the four most recent QRS complexes.

After finding the location of a QRS complex based on output from $Y_{MWI}$ signal, the algorithm searches for R wave peak in $Y_{ECG}$ signal. The preprocessing of ECG signal introduces a delay in locations of maxima (peaks) in $Y_{MWI}$ signal relative to locations of R wave peaks in $Y_{ECG}$ signal, therefore, the search for an R wave peak is performed up to 30 samples backwards from the corresponding local maximum in $Y_{MWI}$ signal (the interval of 30 samples was determined empirically and is valid for sampling frequency of 200 Hz). The search of R wave peak takes into account sharply concave morphology of the R wave around the R peak. A sequence of 5 positive and 3 negative or zero first derivatives are therefore sought for. The location of R wave peak is then determined as the location of the sample from $Y_{ECG}$ signal with the maximum value among the samples from which the sequence of 5 positive and 3 negative derivatives was derived. In the same way, the amplitude of the R wave peak is searched for from $Y_{BPF}$ signal because baseline drift was eliminated from this signal and thus included more reliable information about the R wave amplitude.

After the location and amplitude of R wave peak are determined, location of Q wave peak is sought for. The Q wave peak corresponds to a minimum value of Q wave which typically has convex morphology. In order to reliably detect Q wave peak in presence of high-frequency noise frequently encountered in ECG signals, we first applied a 10th-order low-pass Butterwort filter on 50-samples-long ECG segment from $Y_{ECG}$ signal backwards from the R wave peak location (the interval of 50 samples was determined empirically and is valid for sampling frequency of 200 Hz). From this filtered segment, the algorithm then calculates the first derivative backwards from the R wave peak until it finds a sequence of five successive samples among which the first (counted from the left to the right) has either a negative or zero first derivative and the other four have a positive first derivative. The location of Q wave peak thus corresponds to either the first or the second of these five samples, i.e., to the sample with the minimal amplitude value. If these criteria cannot be met within the 50-sample long segment, the location of the minimal value in this filtered segment is taken as the location of Q wave peak.

Search for T wave peak location follows, taking into account typically concave morphology of T wave. In order to reliably detect T wave peak in presence of high-frequency noise frequently encountered in ECG signals, we first applied a 2nd-order low-pass Butterwort filter on a 120-samples-long ECG segment from $Y_{ECG}$ signal forwards from the R wave peak location (the interval of 120 samples was determined empirically and is valid for sampling frequency of 200 Hz). The algorithm calculates the first derivative forwards from the R wave peak until it finds six successive signal samples among which the first four have positive first derivative, the fifth has either a negative or zero first derivative, and the sixth has negative derivative. The location of T wave peak corresponds to the sample with the maximal amplitude value. If these criteria cannot be fulfilled within the 120-sample segment, the location of the maximal value in this filtered segment is taken as the location of T wave peak.

#### 2.1.3.2. The classification submodule.
The most important characteristic of the classification submodule is its ability to distinguish between normal and abnormal (i.e., abnormal heart rhythm or ECG shape) heartbeats. The classification is made based on evaluation of heart rhythm and amplitude of the R wave peak. For evaluation of the heart rhythm, the instantaneous RR interval ($RR$) is compared to the running average of the last four normal RR intervals ($RR_{th}$).
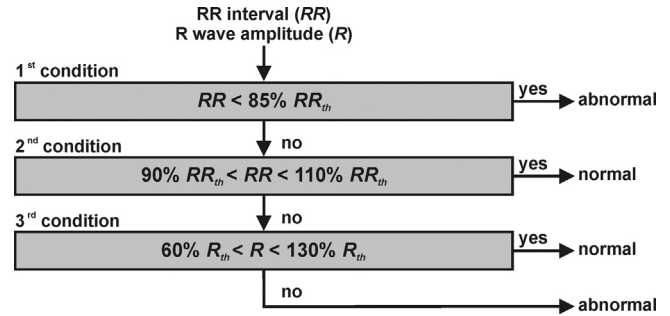


**Fig. 2.** Classification of heartbeats based on values of RR interval and R wave amplitude.

Normal RR interval is determined as interval between two R waves belonging to normal heartbeats. The evaluation of the amplitude of R wave peak is based on comparing the instantaneous amplitude of R wave peak ($R$) to the running average of R wave amplitudes ($R_{th}$) of the last four normal heartbeats. The initial value of parameters $RR_{th}$ and $R_{th}$ is taken from the part II of the learning module.

Classification of a current heartbeat as either normal or abnormal is performed by considering three conditions as shown in Fig. 2. First, if the value of the current RR interval ($RR$) is less than 85% of the average value $RR_{th}$, the heartbeat is classified as abnormal, because it is considered to be too short for normal heart rhythm [50]. Second, if the current value of $RR$ lies within 90–110% of $RR_{th}$, the heartbeat is classified as normal. Third, if the current amplitude of R wave peak ($R$) is within 60–130% of the average value $R_{th}$, the heartbeat is considered to be normal, otherwise it is considered to be abnormal. The classification limits were previously empirically determined [51,52].

These three classification conditions work well if values of $RR_{th}$ and $R_{th}$ are regularly and correctly updated by dropping the oldest and including the newest RR interval or R wave amplitude respectively in the corresponding running average. $RR_{th}$ is updated if the value of the current $RR$ is within 75–125% of the current $RR_{th}$. $R_{th}$ is updated with the current R wave amplitude if the value of $R$ is within 60–140% of the current $R_{th}$. The conditions for updating are less strict than from the conditions used for classification (see Fig. 2) which allows the algorithm to adapt fast to changes in R wave amplitude and in heart rhythm. A special case occurs when an individual heartbeat classified as abnormal is followed by a heartbeat classified as normal. In this case $RR_{th}$ is updated using the mean average value of the abnormal and the normal heartbeat, provided that this average is within the 90–110% range of the current $RR_{th}$. This exception is important because more such sequences (an abnormal heartbeat followed by a normal one) appearing one after another (like in case of ventricular bigeminy) can lead to a slightly increased heart rate. So if these slightly shorter RR intervals were not used to update the $RR_{th}$, the $RR_{th}$ could gradually become an inaccurate estimation of the heart rate and could lead to misclassification of normal heartbeats as abnormal.

#### 2.1.4. Selection and verification module
##### 2.1.4.1. Selection of ECG segments for data analysis.
In case of relatively long ECG signals (i.e., more than several hours long) it might not be necessary to analyze the entire ECG signal, as the analysis of only a selection of short segments from the original ECG signal might be sufficient. In our software, the user can choose between manual and automated selection of ECG segments for data analysis. In the manual mode, the starting point and duration of ECG segments that will be included into analysis can be selected manually. In automated mode, ECG segments for data analysis can be selected from original ECG signal by setting values of the following four selection parameters (criteria): the mean frequency of ECG

segment selection (e.g., one segment per 20 min); the length of ECG segment, which has to be shorter than the mean duration between ECG segments (defined with mean frequency of ECG segment selection) (e.g., 5 min); the maximal allowable percentage of abnormal heartbeats (as identified with detection and classification module) in each ECG segment; and the minimal required time interval between two successive selected ECG segments. According to the recommendations in the literature for short-term ECG recordings [53], the commonly used length of selected short-term ECG segments is 5 min. If no ECG segment can be selected according to these four criteria, the criterion for allowed percentage of abnormal heartbeats is increased by 1% up to maximum 5% until such segment can be determined. The upper limit of 5% was adopted from Salo et al. where authors analyzed the effects of editing abnormal heartbeats on calculation of HRV measures, and showed that if 5% of abnormal heartbeats are present in the analyzed ECG segment, the relative error in calculation of HRV measures can be expected to be less than 5% [54]. This conservative upper limit is used in the current version of our software, even though there are some indications that this limit could be relaxed to 10% without serious deterioration in quality of HRV parameters [55].

*2.1.4.2. Verification of ECG feature points.* Once the ECG segments have been selected, these ECG segments (and not the entire original ECG signal) can be visually reviewed for correctness of R wave peak detection and heartbeat classification and, if necessary, manually corrected to assure correct identification and classification of every single heartbeat. After screening and editing of locations and classifications of R wave peak, the locations of Q and T wave peaks can also be verified but only for heartbeats classified as normal since locations of Q and T wave peaks of abnormal heartbeats do not exist or are unreliable and thus inappropriate for the analysis. At the end of this visual screening of ECG feature points, the so-called verified ECG feature points are determined (see Fig. 1).

### 2.1.5. ECG and HRV analysis module

In this module, ECG and HRV parameters are calculated and statistical analysis of the results is performed.

Each heartbeat can be characterized by several typical ECG parameters, such as P, R and T wave amplitudes, level of ST segment, and RR and QT intervals. Values of these ECG parameters provide information about several cardiac dysfunctions. RR and QT intervals are the most important parameters for diagnosis of arrhythmias. In addition to these two, R wave amplitude can be used for distinction between normal and abnormal heartbeats or between heartbeats and artifacts. R wave amplitude is also a parameter for distinction between atrial and ventricular premature beats. Because the rhythm disturbances can already be reliably evaluated using R wave amplitude and RR and QT interval, at this stage, we included evaluation of only these ECG parameters in our tool. The standard QT interval is defined as the time interval between the start of Q wave and the end of T wave. In our software tool, the peak-to-peak QT interval (ppQT; an interval between the Q wave peak and the T wave peak occurrence within each individual normal heartbeat) was used instead of the standard QT interval because the Q and T wave peaks can be determined more reliably than the start of Q wave and the end of T wave. The corrected ppQT interval (denoted as ppQTc interval) was determined for each heartbeat as the ppQT interval divided by the square root of the corresponding RR interval (a definition analogous to that of the standard corrected QT interval).

After classification and visual verification of heartbeats within the selected ECG segments, HRV analysis can be performed. HRV analysis is based on analysis of fluctuations of the so-called normal-to-normal (NN) intervals, the RR intervals originating in sinoatrial node [53]. The RR interval sequences obtained from ambulatory ECG recordings may also contain abnormal RR intervals. Inclusion of abnormal RR intervals in HRV analysis, however, affects substantially the results of the time-domain and especially the frequency-domain HRV analysis [53]. Therefore, additional pre-processing of the RR interval sequence is needed before the HRV analysis.

In our software tool, sections including abnormal heartbeats are edited using cubic spline interpolation method, where each abnormal RR interval is replaced with the interpolated RR interval. Cubic spline interpolation proved to be a more reliable method than deletion of abnormal RR intervals [56]. By applying this method, NN interval sequence appropriate for HRV analysis is obtained. The NN interval sequence is an irregularly sampled time sequence. For spectral analysis it must therefore be converted to an equidistantly sampled sequence. We applied cubic spline interpolation method at 1000 Hz sample rate and then resampled the interpolated NN interval sequence at 4 Hz [53]. This equidistantly sampled NN interval sequence was finally used for assessment of HRV.

Following the recommendations in the literature for short-term ECG recordings [53], several HRV parameters in time-domain (mean NN, SDNN, SDSD, RMSSD, pNN50) and frequency-domain (LF, nLF, HF, nHF, LF/HF), and nonlinear measures, i.e., Poincaré descriptors (SD1, SD2, SD1/SD2) can be calculated using our software tool for each ECG segment included in the analysis (for description of these parameters see Table 1). In order to remove the low frequency baseline trend component in the NN interval sequence, the linear detrending of each NN interval sequence is also applied before calculation of HRV parameters (except for the mean NN parameter and the Poincaré descriptors). Frequency-domain HRV parameters are calculated with parametric autoregressive (AR) model of the order 16 with coefficients determined based on Burg method which provides more accurate estimation of spectrum and easier automated calculation of frequency power components than non-parametric methods based on Fourier transform [53,57].

After all ECG and HRV parameters are calculated for all ECG segments, statistical analysis of these parameters can be performed. At this stage of development of our software tool, values of mean, standard deviation, median, range, percentile, and number and percentage of normal and abnormal heartbeats are calculated.

## 2.2. Evaluation of heartbeat detection and classification

### 2.2.1. ECG database

We evaluated the performance of R wave peak detection and heartbeat classification using 19 sample ECG records of the Long-Term ST database (LTST database) [58]. These records contain 2-hour-long ambulatory ECG signals, which include abnormal heartbeats of various pathological backgrounds. All heartbeats in these signals were classified and annotated by experts. The performance of Q and T wave peak detection of our software was not evaluated at this point due to unavailability of ECG signals with verified Q and T wave peak annotations but this evaluation is planned for the future.

### 2.2.2. Performance metrics

For evaluation of the QRS detection algorithm, we calculated the following scores for each sample ECG record:

- $N_{qrs}$, the total number of all QRS complexes (normal and abnormal), i.e., the sum of $TP_{qrs}$ and $FN_{qrs}$;
- $TP_{qrs}$, the true positive for QRS detection, i.e., the number of correctly detected QRS complexes;
- $FN_{qrs}$, the false negative for QRS detection, i.e., the number of missed QRS complexes; and

**Table 1**
ECG and HRV parameters currently included in our software tool.

| Parameter | Unit | Description |
|---|---|---|
| *ECG parameters* | | |
| RR | ms | Interval between two R waves |
| NN | ms | Interval between two R waves belonging to normal heartbeats; normal-to-normal interval |
| R amplitude | mV | Amplitude of R wave |
| ppQT | ms | Peak-to-peak QT interval |
| ppQTc | $ms^{1/2}$ | Corrected ppQT interval (ppQT divided by the square root of the corresponding RR interval) |
| *Time-domain HRV parameters* | | |
| mean NN | ms | Mean of normal-to-normal (NN) intervals |
| SDNN | ms | Standard deviation of NN intervals; estimate of overall HRV |
| SDSD | ms | Standard deviation of differences between adjacent NN intervals; estimate of short-term HRV; describes parasympathetic activity |
| RMSSD | ms | Square root of the mean of the sum of the squares of differences between adjacent NN intervals; estimate of short-term HRV; describes parasympathetic activity |
| pNN50 | % | Number of pairs of adjacent NN intervals differing by more than 50 ms divided by the total number of all NN intervals |
| *Nonlinear HRV parameters* | | |
| SD1 | ms | Standard deviation of the Poincaré plot perpendicular to line-of-identity; shortest diameter of the fitted ellipse; estimate of short-term HRV; describes parasympathetic activity |
| SD2 | ms | Standard deviation of the Poincaré plot along the line-of-identity; largest diameter of the fitted ellipse; estimate of long-term HRV; describes sympathetic activity |
| SD1/SD2 | – | Ratio of SD1 to SD2; describes the ratio of short-term to long-term HRV; describes the ratio between parasympathetic and sympathetic activity |
| *Frequency-domain HRV parameters* | | |
| LF | $ms^2$ | Power in low frequency range (0.04–0.15 Hz); estimate of long-term HRV; reflects both sympathetic and parasympathetic activity |
| nLF | n.u. | Normalized power of LF; LF/(LF + HF) × 100; estimate of long-term HRV; reflects both sympathetic and parasympathetic activity |
| HF | $ms^2$ | Power in high frequency range (0.15–0.4 Hz); estimate of short-term HRV; describes parasympathetic (vagal) activity |
| nHF | n.u. | Normalized power of HF; HF/(LF + HF) × 100; estimate of short-term HRV; describes parasympathetic activity |
| LF/HF | – | Ratio between LF and HF range powers; describes the ratio of long-term to short-term HRV; describes the ratio between sympathetic and parasympathetic activity, i.e., sympathovagal balance |

– $FP_{qrs}$, the false positive for QRS detection, i.e., the number of false QRS detections.

For evaluation of the classification algorithm, we used the following additional scores for each record:

– $N_n$, the total number of normal heartbeats in the database, i.e., the sum of $TP_n$ and $FN_n$;
– $TP_n$, the true positive for classification, i.e., the number of correctly classified normal heartbeats;
– $FN_n$, the false negative for classification, i.e., the number of missed normal heartbeats; and
– $FP_n$, the false positive for classification, i.e., they can arise both from correctly detected but erroneously classified QRS

complexes (a subgroup of $TP_{qrs}$) and from erroneously detected QRS complexes (a subgroup of $FP_{qrs}$).

Based on these scores obtained with a beat-by-beat comparison of the results of our algorithm with true human-expert annotations of the heartbeats defined in the LTST database, we calculated standard performance measures for QRS detection: sensitivity ($Se_{qrs}(\%) = 100 \cdot TP_{qrs}/N_{qrs}$), positive predictivity ($+P_{qrs}(\%) = 100 \cdot TP_{qrs}/(TP_{qrs} + FP_{qrs})$) and detection error rate ($DER_{qrs}(\%) = 100 \cdot (FP_{qrs} + FN_{qrs})/N_{qrs}$) for QRS detection. Similarly, we defined performance measures for classification of normal heartbeats: sensitivity ($Se_n(\%) = 100 \cdot TP_n/N_n$), positive predictivity ($+P_n(\%) = 100 \cdot TP_n/(TP_n + FP_n)$) and classification error rate ($DER_n(\%) = 100 \cdot FP_n/N_n$) for normal heartbeats.

### 2.2.3. Programming
The software tool and all routines for evaluation of performance of the algorithm were written in Matlab and implemented on a PC platform.

## 3. Results

We developed a Matlab-based GUI-driven tool for reliable and effective detection and classification of heartbeats from ECG signals and calculation of ECG and HRV parameters. For the structure of the tool see Fig. 1.

A software tool provides the following functionalities: automated selection of ECG segments from ECG signal according to selection restrictions; automated detection of prominent heartbeat features, such as Q, R and T wave peak; automated classification of individual heartbeat as normal or abnormal; displaying annotations of detections and classifications of heartbeat features; quick manual screening of analyzed ECG signal; and manual corrections of annotation and classification errors. Special software tool with graphical user interface was developed for easier screening and verification of the located feature points (Q, R and T wave peaks) and classification of heartbeats (Fig. 3).

The NN interval sequence is built from verified locations of R wave peaks and classifications obtained from the screening process. All abnormal RR intervals are automatically replaced with calculated normal RR intervals based on cubic spline interpolation method.

The algorithm's performance for QRS detection and classification is summarized in Table 2. We provide a statistical summary of the results using both the mean and standard deviation and the median and quartile values. However, when we say 'on average' in the text we are referring to median values, because the data were not normally distributed. On average, the algorithm correctly detected 99.78% of all QRS complexes ($Se_{qrs}$). The total number of erroneously detected QRS complexes was 338 which is a small number compared to the total number of QRS complexes analyzed (over 160,000). The average detection error rate ($DER_{qrs}$) and positive predictivity ($+P_{qrs}$) of QRS detection were 0.35% and 99.98%, respectively. On average, the algorithm correctly classified 99.45% of normal QRS complexes ($Se_n$). The average error rate ($DER_n$) and the positive predictivity ($+P_n$) of normal heartbeat classification were 0.01% and 99.99%, respectively.

## 4. Discussion

This paper discusses the functionality and performance evaluation of a software tool for detection and classification of heartbeats and calculation of ECG and HRV parameters.

The software tool is a significant improvement over other available software in the field of HRV analysis, because it incorporates
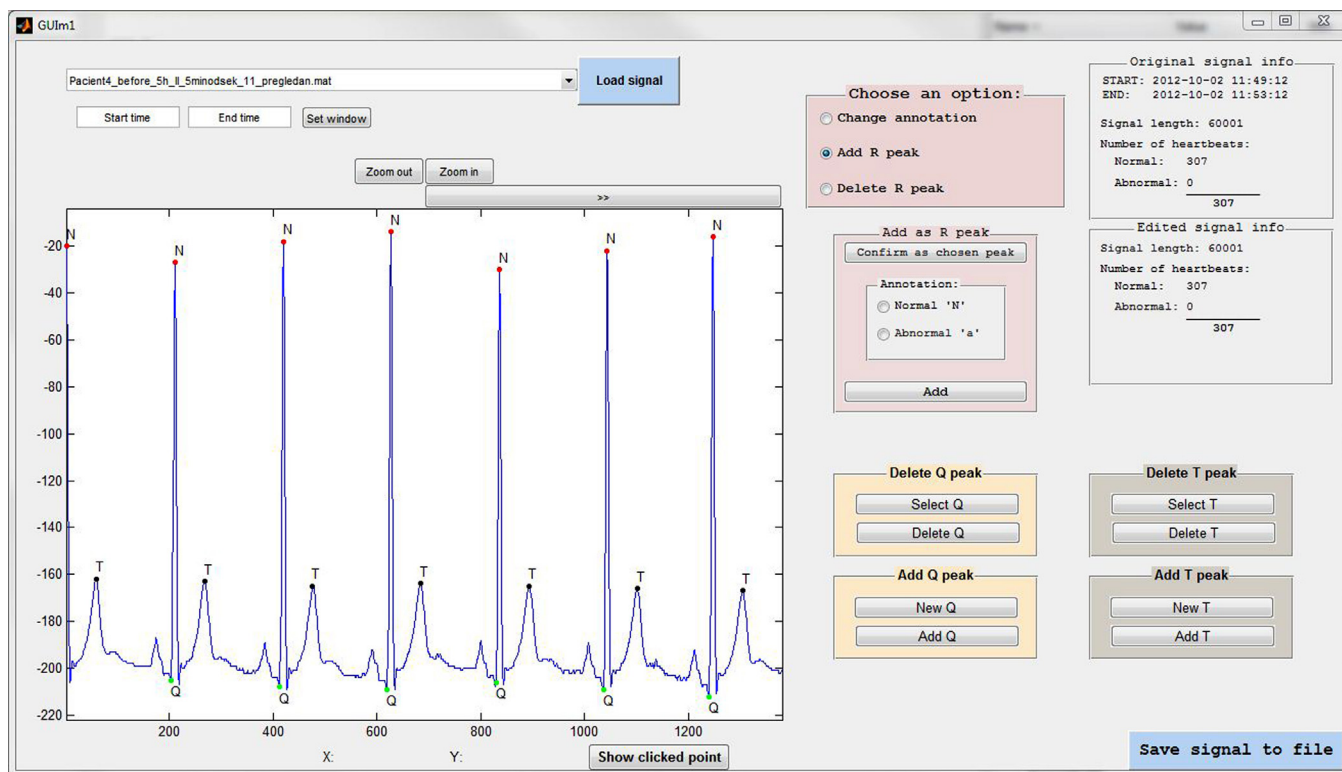
**Fig. 3.** Graphical user interface for screening and verification of Q, R and T wave peak locations. At the top, ECG signal for editing is selected and loaded. ECG signal is plotted and can be zoomed in or out and advanced along the time axis in either direction, which allows editing of ECG signal segment by segment. Q, R and T wave peak locations can be deleted or added. The annotation for R wave peak location can also be changed from normal to abnormal or vice versa. In the upper right corner, the information about the original and the edited ECG signal is displayed (i.e., about the start and the end of absolute recording time of ECG signal, total length of ECG signal in samples, and number of normal and abnormal heartbeats detected within the ECG signal). After editing of Q, R and T wave peaks, the changes can be saved in a separate file.

the functionality for automated selection of the most adequate ECG segments from ECG signal for HRV analysis. To the best of our knowledge, no tool available on the market includes such built-in module for automated selection. This property of the tool enables extraction of relatively noise-free ECG segments that are the most suitable for reliable HRV analysis and presents important characteristics in terms of objective, unbiased and quick selection of ECG segments.

The fundamental functionality of the tool is reliable detection of QRS complexes which in comparison to other software tools for HRV analysis is not a frequently implemented characteristics, for example Kubios does not provide QRS detection at all. The QRS detection algorithm has to correctly detect as many as possible heartbeats (high $TP_{qrs}$ and $Se_{qrs}$) without false positive QRS detections (low $FP_{qrs}$). When testing our QRS detection algorithm on 19 sample ECG signals from the LTST database (with relatively low level of high-frequency noise present), the algorithm fulfilled these requirements excellently as indicated by practically ideal $Se_{qrs}$ and $+P_{qrs}$ values (Table 2). The performance of our QRS detection algorithm approached the ideal level at a degree similar to that of some other detectors with comparably simple algorithms [59–61]. The records with poorest results of our algorithm (having large $DER_{qrs}$) contain a transient appearance of high-frequency noise with amplitudes similar to that of the R wave (typical examples: records 119, 139 and 159). At this stage of development, our algorithm is not well suited to deal with signals that have very low signal-to-noise ratio or are largely nonstationary. We do not find this to be critical because for such signals only the ECG segments with relatively low level of noise can be selected for the analysis (by defining suitable selection criteria for the automated selection of ECG segments from ECG signal; see Section 2.1.4.1) or manual detection and classification of heartbeats can be performed in critical parts of the ECG

signal. However, the algorithm deals well with mildly nonstationary parts of the signal or transient onsets of noise contamination with low amplitudes, which were occasionally encountered in most of the signals used in evaluation of the algorithm. Moreover, many of the false negative QRS detections ($FN_{qrs}$) were present due to very strict requirements for no false positive QRS detections ($FP_{qrs}$). We wanted to achieve the number of $FP_{qrs}$ as low as possible since a false positive is more detrimental for performance of the detection algorithm than a false negative because of the effect on updating of the algorithm's parameters.

The software tool has to correctly classify as many normal heartbeats as possible (high $TP_n$ and $Se_n$) without false positive classifications for normal heartbeats (low $FP_n$ and $DER_n$ and high $+P_n$). Again the false positives are more detrimental to the performance of classification and further on to HRV analysis than the false negatives. The classification algorithm satisfied these requirements excellently as indicated by practically ideal $Se_n$ and $+P_n$ values (Table 2). There were 39 false positive classifications ($FP_n$) in comparison to approximately 160,000 correctly classified normal heartbeats in evaluated ECG signals. The reason for these erroneously classified heartbeats is mainly in particular arrhythmias that are sometimes indistinguishable from the normal heartbeats in terms of morphology or the time of appearance. However, even though algorithm erroneously classifies some normal heartbeats, these mistakes can be manually corrected in further evaluation steps of the tool, i.e., during the screening of ECG segments. It should be pointed out that presently the parameters $Se_n$, $+P_n$ and $DER_n$ (Table 2) reflect a combined performance of both the detection algorithm and the classification algorithms. We justify this by the fact that both these components were fine-tuned together and not independently of each other because of our specific final application of our tool. In the future, however, we intend to separate

**Table 2**
Performance measures for QRS detection and heartbeat classification.

| Signal[a] | Original data | | | Detection of heartbeats | | | | | | Detection & classification of normal heartbeats | | | | | |
|---|---|---|---|---|---|---|---|---|---|---|---|---|---|---|---|
| | $N_{qrs}$ | $N_n$ | $N_a$ | $TP_{qrs}$ | $FN_{qrs}$ | $FP_{qrs}$ | $Se_{qrs}$ (%) | $+P_{qrs}$ (%) | $DER_{qrs}$ (%) | $TP_n$ | $FN_n$ | $FP_n$ | $Se_n$ (%) | $+P_n$ (%) | $DER_n$ (%) |
| 103 | 7279 | 7195 | 84 | 7251 | 28 | 0 | 99.62 | 100.00 | 0.38 | 7176 | 19 | 5 | 99.74 | 99.93 | 0.07 |
| 105 | 6615 | 6613 | 2 | 6607 | 8 | 3 | 99.88 | 99.95 | 0.17 | 6582 | 31 | 2 | 99.53 | 99.97 | 0.03 |
| 107 | 7015 | 7001 | 14 | 6964 | 51 | 10 | 99.27 | 99.86 | 0.87 | 6929 | 72 | 1 | 98.97 | 99.99 | 0.01 |
| 111 | 7519 | 7518 | 1 | 7494 | 25 | 1 | 99.67 | 99.99 | 0.35 | 7469 | 49 | 0 | 99.35 | 100.00 | 0.00 |
| 113 | 8929 | 8911 | 18 | 8915 | 14 | 0 | 99.84 | 100.00 | 0.16 | 8865 | 46 | 1 | 99.48 | 99.99 | 0.01 |
| 119 | 7702 | 7701 | 1 | 7647 | 55 | 35 | 99.29 | 99.54 | 1.17 | 7600 | 101 | 0 | 98.69 | 100.00 | 0.00 |
| 121 | 10,609 | 10,594 | 15 | 10,590 | 19 | 30 | 99.82 | 99.72 | 0.46 | 10,534 | 60 | 5 | 99.43 | 99.95 | 0.05 |
| 123 | 9155 | 9149 | 6 | 9136 | 19 | 1 | 99.79 | 99.99 | 0.22 | 9110 | 39 | 0 | 99.57 | 100.00 | 0.00 |
| 125 | 9047 | 9043 | 4 | 9024 | 23 | 2 | 99.75 | 99.98 | 0.28 | 8997 | 46 | 0 | 99.49 | 100.00 | 0.00 |
| 127 | 9373 | 9373 | 0 | 9373 | 0 | 0 | 100.00 | 100.00 | 0.00 | 9349 | 24 | 0 | 99.74 | 100.00 | 0.00 |
| 139 | 10,611 | 10,611 | 0 | 10,504 | 107 | 48 | 98.99 | 99.55 | 1.46 | 10,288 | 323 | 0 | 96.96 | 100.00 | 0.00 |
| 147 | 6360 | 6357 | 3 | 6354 | 6 | 0 | 99.91 | 100.00 | 0.09 | 6326 | 31 | 3 | 99.51 | 99.95 | 0.05 |
| 155 | 8106 | 8105 | 1 | 8088 | 18 | 15 | 99.78 | 99.81 | 0.41 | 8050 | 55 | 0 | 99.32 | 100.00 | 0.00 |
| 159 | 9180 | 9131 | 49 | 8900 | 280 | 184 | 96.95 | 97.97 | 5.05 | 8820 | 311 | 1 | 96.59 | 99.99 | 0.01 |
| 161 | 8841 | 8836 | 5 | 8840 | 1 | 1 | 99.99 | 99.99 | 0.02 | 8787 | 49 | 0 | 99.45 | 100.00 | 0.00 |
| 163 | 7599 | 7586 | 13 | 7595 | 4 | 3 | 99.95 | 99.96 | 0.09 | 7565 | 21 | 2 | 99.72 | 99.97 | 0.03 |
| 501 | 7739 | 7734 | 5 | 7728 | 11 | 1 | 99.86 | 99.99 | 0.16 | 7701 | 33 | 1 | 99.57 | 99.99 | 0.01 |
| 509 | 8074 | 7928 | 146 | 8005 | 69 | 2 | 99.15 | 99.98 | 0.88 | 7876 | 52 | 3 | 99.34 | 99.96 | 0.04 |
| 607 | 10,248 | 10,200 | 48 | 10,197 | 51 | 2 | 99.50 | 99.98 | 0.52 | 10,131 | 69 | 15 | 99.32 | 99.85 | 0.15 |
| Total | 160,001 | 159,586 | 415 | 159,212 | 789 | 338 | – | – | – | 158,155 | 1431 | 39 | – | – | – |
| Min | 6360 | 6357 | 0 | 6354 | 0 | 0 | 96.95 | 97.97 | 0.00 | 6326 | 19 | 0 | 96.59 | 99.85 | 0.00 |
| 25% | 7519 | 7518 | 1 | 7494 | 8 | 1 | 99.29 | 99.81 | 0.16 | 7469 | 31 | 0 | 99.32 | 99.96 | 0.00 |
| Median | 8106 | 8105 | 5 | 8088 | 19 | 2 | 99.78 | 99.98 | 0.35 | 8050 | 49 | 1 | 99.45 | 99.99 | 0.01 |
| 75% | 9180 | 9149 | 18 | 9136 | 51 | 15 | 99.88 | 99.99 | 0.87 | 9110 | 69 | 3 | 99.57 | 100.00 | 0.04 |
| Max | 10,611 | 10,611 | 146 | 10,590 | 280 | 184 | 100.00 | 100.00 | 5.05 | 10,534 | 323 | 15 | 99.74 | 100.00 | 0.15 |
| Mean | 8421 | 8399 | 22 | 8380 | 42 | 18 | 99.53 | 99.80 | 0.67 | 8324 | 75 | 2 | 99.15 | 99.98 | 0.02 |
| Std | 1241 | 1242 | 36 | 1226 | 62 | 41 | 0.67 | 0.45 | 1.10 | 1207 | 85 | 3 | 0.85 | 0.04 | 0.04 |
| $CI_{95\%LL}$ | 7863 | 7841 | 6 | 7828 | 14 | 0 | 99.22 | 99.60 | 0.17 | 7781 | 37 | 1 | 98.76 | 99.96 | 0.01 |
| $CI_{95\%UL}$ | 8979 | 8958 | 38 | 8931 | 69 | 36 | 99.83 | 100.00 | 1.17 | 8867 | 114 | 4 | 99.53 | 99.99 | 0.04 |

[a] Names of ECG signals are original names from LTST database; $N_{qrs}$, the total number of possible detected QRS complexes (normal and abnormal, $N_n$ and $N_a$), i.e., the sum of $TP_{qrs}$ and $FN_{qrs}$; $N_n$, the total number of normal heartbeats, i.e., the sum of $TP_n$ and $FN_n$; $N_a$, the total number of abnormal heartbeats; $TP_{qrs}$, the true positive for QRS detection, i.e., the number of correctly detected QRS complexes; $FN_{qrs}$, the false negative for QRS detection, i.e., the number of missed QRS complexes; $FP_{qrs}$, the false positive for QRS detection, i.e., the number of false QRS detections; $Se_{qrs}$ = sensitivity for QRS detection; $+P_{qrs}$ = positive predictivity for QRS detection; $DER_{qrs}$ = detection error rate for QRS detection; $TP_n$, the true positive for classification, i.e., the number of correctly classified normal heartbeats; $FN_n$, the false negative for classification, i.e., the number of missed normal heartbeats; $FP_n$, the false positive for classification; $Se_n$ = sensitivity for normal heartbeats; $+P_n$ = positive predictivity for normal heartbeats; $DER_n$ = detection error rate for normal heartbeats; $CI_{95\%LL}$ = lower limit of 95% confidence interval; $CI_{95\%UL}$ = upper limit of 95% confidence interval.

evaluation of the two algorithms and also to assess the classification performance with respect to different types of arrhythmias present in ECG records.

Beside the module for reliable QRS detection and heartbeat classification, our tool incorporates selection and verification module. This module displays automatically detected heartbeats with annotated and classified R wave peaks and detected Q and T wave peaks. In addition, it enables quick manual screening of ECG segments selected for evaluation, and manual corrections of erroneously detected or classified heartbeats or wave peaks (Fig. 3). These functionalities of our software tool present useful and time-saving characteristics since the screening and correction processes are always a tedious and time-consuming work. Moreover, our tool does not require a clear RR sequence based on only normal heartbeats. The NN sequence is built after verification of ECG feature points when all potential abnormal RR intervals are automatically replaced with interpolated normal NN intervals.

The described software tool for detection and classification of heartbeats and calculation of ECG and HRV parameters presents a significant improvement over other available software (such as Kubios, SyneScope, Biopac, Nevrokard HRV system) in the field of HRV analysis, because it incorporates a unique set of functionalities among which some are not at all or only rarely individually provided in commonly available software but, to the best of our knowledge, no software tool available on the market provides all of them. The distinctive functionalities that our software tool provides are: (1) reliable and automated detection of QRS and other prominent heartbeat features, such as Q, R and T wave peak; (2) automated selection of the most adequate ECG segments from ECG signal for HRV analysis according to specific user-defined requirements; (3) automated classification of individual heartbeat as normal or abnormal; (4) displaying of heartbeat annotations; (5) quick manual screening of analyzed ECG signal; and (6) manual correction of annotation and classification errors.

## 5. Conclusions

We tested the performance of a newly designed software tool for reliable and effective detection and classification of heartbeats and calculation of ECG and HRV parameters. This tool will serve in clarification of issues concerning patient safety during the electroporation-based treatments used in clinical practice, such as electrochemotherapy, electrotransfer for gene therapy and DNA vaccination and non-thermal irreversible electroporation. Electric pulses used in electroporation-based treatments are of very high intensities (voltages up to several kilovolts, currents up to several tens of amperes) and can potentially induce heart-related effects in spite of their very short durations [44,46,52]. Safety considerations are becoming increasingly important because new applications of electroporation-based treatments using endoscopic, percutaneous or surgical means to access internal tumors or tissues are being developed. Due to relatively large electrical conductivity of internal tissues and organs [62] and pronounced nonlinear tissue characteristics [63,64], electroporation pulses in these new treatment modalities might have an increased probability of affecting cardiac muscle and thus greater potential of inducing heart-related effects, especially when the application zone is in immediate vicinity of the heart [15,38,41–48]. Our software tool represents a significant improvement over the existing practice of evaluation of changes in functioning of the heart due to electroporation-based treatments. This software tool can of course also be used for evaluation of changes in ECG or HRV parameters in other applications where the effects of clinical interventions (e.g., effects of drugs) or different physiological conditions (e.g., effects of anxiety or stress) are investigated.

## Conflicts of interest

Authors declare no conflicts of interests.

## References

[1] J.C. Weaver, Y.A. Chizmadzhev, Theory of electroporation: a review, Bioelectrochem. Bioenerg. 41 (1996) 135–160.
[2] J.C. Weaver, Electroporation of cells and tissues, IEEE Trans. Plasma Sci. 28 (2000) 24–33.
[3] C. Chen, S.W. Smye, M.P. Robinson, J.A. Evans, Membrane electroporation theories: a review, Med. Biol. Eng. Comput. 44 (2006) 5–14.
[4] T. Kotnik, P. Kramar, G. Pucihar, D. Miklavcic, M. Tarek, Cell membrane electroporation – Part 1: The phenomenon, IEEE Electr. Insul. Mag. 28 (2012) 14–23.
[5] L.M. Mir, S. Orlowski, J. Belehradek Jr., C. Paoletti, Electrochemotherapy potentiation of antitumour effect of bleomycin by local electric pulses, Eur. J. Cancer 27 (1991) 68–72.
[6] A. Macek Lebar, G. Sersa, S. Kranjc, A. Groselj, D. Miklavcic, Optimisation of pulse parameters in vitro for in vivo electrochemotherapy, Anticancer Res. 22 (2002) 1731–1736.
[7] A. Zupanic, S. Corovic, D. Miklavcic, Optimization of electrode position and electric pulse amplitude in electrochemotherapy, Radiol. Oncol. 42 (2008) 93–101.
[8] M. Cemazar, M. Golzio, G. Sersa, P. Hojman, S. Kranjc, S. Mesojednik, et al., Control by pulse parameters of DNA electrotransfer into solid tumors in mice, Gene Ther. 16 (2009) 635–644.
[9] D. Miklavcic, L. Towhidi, Numerical study of the electroporation pulse shape effect on molecular uptake of biological cells, Radiol. Oncol. 44 (2010) 34–41.
[10] D. Miklavcic, M. Snoj, A. Zupanic, B. Kos, M. Cemazar, M. Kropivnik, et al., Towards treatment planning and treatment of deep-seated solid tumors by electrochemotherapy, Biomed. Eng. Online 9 (2010) 10.
[11] S. Haberl, D. Miklavcic, G. Sersa, W. Frey, B. Rubinsky, Cell membrane electroporation – Part 2: The applications, IEEE Electr. Insul. Mag. 29 (2013) 29–37.
[12] M. Marty, G. Sersa, J.R. Garbay, J. Gehl, C.G. Collins, M. Snoj, et al., Electrochemotherapy – an easy, highly effective and safe treatment of cutaneous and subcutaneous metastases: results of ESOPE (European Standard Operating Procedures of Electrochemotherapy) study, Eur. J. Cancer Suppl. 4 (2006) 3–13.
[13] M.G. Moller, S. Salwa, D.M. Soden, G.C. O'Sullivan, Electrochemotherapy as an adjunct or alternative to other treatments for unresectable or in-transit melanoma, Expert Rev. Anticancer Ther. 9 (2009) 1611–1630.
[14] T. Hampton, Electric pulses help with chemotherapy, may open new paths for other agents, JAMA 305 (2011) 549–551.
[15] I. Edhemovic, E.M. Gadzijev, E. Brecelj, D. Miklavcic, B. Kos, A. Zupanic, et al., Electrochemotherapy: a new technological approach in treatment of metastases in the liver, Technol. Cancer Res. Treat. 10 (2011) 475–485.
[16] G. Sersa, T. Cufer, S.M. Paulin, M. Cemazar, M. Snoj, Electrochemotherapy of chest wall breast cancer recurrence, Cancer Treat. Rev. 38 (2012) 379–386.
[17] L.G. Campana, S. Valpione, S. Mocellin, R. Sundararajan, E. Granziera, L. Sartore, et al., Electrochemotherapy for disseminated superficial metastases from malignant melanoma, Br. J. Surg. 99 (2012) 821–830.
[18] B. Mali, T. Jarm, M. Snoj, G. Sersa, D. Miklavcic, Antitumor effectiveness of electrochemotherapy: a systematic review and meta-analysis, Eur. J. Surg. Oncol. 39 (2013) 4–16.
[19] F. Andre, L.M. Mir, DNA electrotransfer: its principles and an updated review of its therapeutic applications, Gene Ther. 11 (2004) S33–S42.
[20] F.M. Andre, J. Gehl, G. Sersa, V. Preat, P. Hojman, J. Eriksen, et al., Efficiency of high- and low-voltage pulse combinations for gene electrotransfer in muscle, liver, tumor, and skin, Hum. Gene Ther. 19 (2008) 1261–1271.
[21] A. Gothelf, J. Gehl, Gene electrotransfer to skin: review of existing literature and clinical perspectives, Curr. Gene Ther. 10 (2010) 287–299.
[22] S.V. Littel-van den Hurk, D. Hannaman, Electroporation for DNA immunization: clinical application, Expert Rev. Vaccines 9 (2010) 503–517.
[23] L.C. Heller, R. Heller, Electroporation gene therapy preclinical and clinical trials for melanoma, Curr. Gene Ther. 10 (2010) 312–317.
[24] P. Hojman, Basic principles and clinical advancements of muscle electrotransfer, Curr. Gene Ther. 10 (2010) 128–138.
[25] M.R. Prausnitz, A practical assessment of transdermal drug delivery by skin electroporation, Adv. Drug Deliv. Rev. 35 (1999) 61–76.
[26] A.R. Denet, R. Vanbever, V. Preat, Skin electroporation for transdermal and topical delivery, Adv. Drug Deliv. Rev. 56 (2004) 659–674.
[27] N. Pavselj, V. Preat, DNA electrotransfer into the skin using a combination of one high- and one low-voltage pulse, J. Controlled Release 106 (2005) 407–415.

[28] H. Kalluri, A.K. Banga, Transdermal delivery of proteins, AAPS Pharm. Sci. Tech. 12 (2011) 431–441.
[29] T.W. Wong, T.Y. Chen, C.C. Huang, J.C. Tsai, S.W. Hui, Painless skin electroporation as a novel way for insulin delivery, Diabetes Technol. Ther. 13 (2011) 929–935.
[30] H. Mekid, L.M. Mir, In vivo cell electrofusion, Biochim. Biophys. Acta 1524 (2000) 118–130.
[31] K. Trontelj, M. Rebersek, M. Kanduser, V.C. Serbec, M. Sprohar, D. Miklavcic, Optimization of bulk cell electrofusion in vitro for production of human-mouse heterohybridoma cells, Bioelectrochemistry 74 (2008) 124–129.
[32] S. Salomskaite-Davalgiene, K. Cepurniene, S. Satkauskas, M.S. Venslauskas, L.M. Mir, Extent of cell electrofusion in vitro and in vivo is cell line dependent, Anticancer Res. 29 (2009) 3125–3130.
[33] M. Usaj, K. Trontelj, D. Miklavcic, M. Kanduser, Cell-cell electrofusion: optimization of electric field amplitude and hypotonic treatment for mouse melanoma (B16-F1) and Chinese Hamster ovary (CHO) cells, J. Membr. Biol. 236 (2010) 107–116.
[34] M. Usaj, K. Flisar, D. Miklavcic, M. Kanduser, Electrofusion of B16-F1 and CHO cells: the comparison of the pulse first and contact first protocols, Bioelectrochemistry 89 (2013) 34–41.
[35] R. Davalos, L. Mir, B. Rubinsky, Tissue ablation with irreversible electroporation, Ann. Biomed. Eng. 33 (2005) 223–231.
[36] B. Rubinsky, Irreversible electroporation in medicine, Technol. Cancer Res. Treat. 6 (2007) 255–259.
[37] E. Maor, A. Ivorra, B. Rubinsky, Non thermal irreversible electroporation: novel technology for vascular smooth muscle cells ablation, PLoS ONE 4 (2009) e4757.
[38] M. Pech, A. Janitzky, J.J. Wendler, C. Strang, S. Blaschke, O. Dudeck, et al., Irreversible electroporation of renal cell carcinoma: a first-in-man phase I clinical study, Cardiovasc. Intervent. Radiol. 34 (2011) 132–138.
[39] C.R. Tracy, W. Kabbani, J.A. Cadeddu, Irreversible electroporation (IRE): a novel method for renal tissue ablation, BJU Int. 107 (2011) 1982–1987.
[40] D. Miklavcic, Network for development of electroporation-based technologies and treatments: COST TD1104, J. Membr. Biol. 245 (2012) 591–598.
[41] W.G. Marshall Jr., B.A. Boone, J.D. Burgos, S.I. Gografe, M.K. Baldwin, M.L. Danielson, et al., Electroporation-mediated delivery of a naked DNA plasmid expressing VEGF to the porcine heart enhances protein expression, Gene Ther. 17 (2010) 419–423.
[42] E.L. Ayuni, A. Gazdhar, M.N. Giraud, A. Kadner, M. Gugger, M. Cecchini, et al., In vivo electroporation mediated gene delivery to the beating heart, PLoS ONE 5 (2010) e14467.
[43] B. Hargrave, H. Downey, R. Strange, L. Murray, C. Cinnamond, C. Lundberg, et al., Electroporation-mediated gene transfer directly to the swine heart, Gene Ther. 20 (2013) 151–157.
[44] C. Ball, K.R. Thomson, H. Kavnoudias, Irreversible electroporation: a new challenge in "out of operating theater" anesthesia, Anesth. Analg. 110 (2010) 1305–1309.
[45] K. Thomson, Human experience with irreversible electroporation, in: B. Rubinsky (Ed.), Irreversible Electroporation, Springer Verlag, Berlin, Heidelberg, 2010, pp. 249–254.
[46] A. Deodhar, T. Dickfeld, G.W. Single, W.C. Hamilton, R.H. Thornton, C.T. Sofocleous, et al., Irreversible electroporation near the heart: ventricular arrhythmias can be prevented with ECG synchronization, Am. J. Roentgenol. 196 (2011) W330–W335.
[47] S. Bagla, D. Papadouris, Percutaneous irreversible electroporation of surgically unresectable pancreatic cancer: a case report, J. Vasc. Interv. Radiol. 23 (2012) 142–145.
[48] D. Miklavcic, G. Sersa, E. Brecelj, J. Gehl, D. Soden, G. Bianchi, et al., Electrochemotherapy: technological advancements for efficient electroporation-based treatment of internal tumors, Med. Biol. Eng. Comput. 50 (2012) 1213–1225.
[49] J. Pan, W.J. Tompkins, A real-time QRS detection algorithm, IEEE Trans. Biomed. Eng. 32 (1985) 230–236.
[50] C. Burghardt, ECG Interpretation Made Incredibly Easy!, fifth ed, Lippincott Williams & Wilkins, USA, 2010.
[51] B. Mali, T. Jarm, F. Jager, D. Miklavcic, An algorithm for synchronization of in vivo electroporation with ECG, J. Med. Eng. Technol. 29 (2005) 288–296.
[52] B. Mali, T. Jarm, S. Corovic, M.S. Paulin-Kosir, M. Cemazar, G. Sersa, et al., The effect of electroporation pulses on functioning of the heart, Med. Biol. Eng. Comput. 46 (2008) 745–757.
[53] A.J. Camm, M. Malik, J.T. Bigger, G. Breithardt, S. Cerutti, R.J. Cohen, et al., Heart rate variability. Standards of measurement, physiological interpretation, and clinical use, Eur. Heart J. 17 (1996) 354–381.
[54] M.A. Salo, H.V. Huikuri, T. Seppänen, Ectopic beats in heart rate variability analysis: effects of editing on time and frequency domain measures, Ann. Non-invasive Electrocardiol. 6 (2001) 5–17.
[55] P. Melillo, M. Bracale, L. Pecchia, Nonlinear heart rate variability features for real-life stress detection. Case study: students under stress due to university examination, Biomed. Eng. Online 10 (2011) 96.
[56] N. Lippman, K.M. Stein, B.B. Lerman, Comparison of methods for removal of ectopy in measurement of heart rate variability, Am. J. Physiol. 267 (1994) H411–H418.
[57] U.R. Acharya, P.K. Joseph, N. Kannathal, C. Bernat, J. Suri, Heart rate variability: a review, Med. Biol. Eng. Comput. 44 (2006) 1031–1051.
[58] F. Jager, A. Taddei, G.B. Moody, M. Emdin, G. Antolic, R. Dorn, et al., Long-term ST database: a reference for the development and evaluation of automated ischaemia detectors and for the study of the dynamics of myocardial ischaemia, Med. Biol. Eng. Comput. 41 (2003) 172–182.
[59] D. Benitez, P.A. Gaydecki, A. Zaidi, A.P. Fitzpatrick, The use of the Hilbert transform in ECG signal analysis, Comput. Biol. Med. 31 (2001) 399–406.
[60] A. Ruha, S. Sallinen, S. Nissilä, A real-time microprocessor QRS detector system with a 1-ms timing accuracy for the measurement of ambulatory HRV, IEEE Trans. Biomed. Eng. 44 (1997) 159–167.
[61] G.M. Friesen, T.C. Jannett, M.A. Jadallah, S.L. Yates, S.R. Quint, H.T. Nagle, A comparison of the noise sensitivity of nine QRS detection algorithms, IEEE Trans. Biomed. Eng. 37 (1990) 85–98.
[62] D. Miklavcic, N. Pavselj, F.X. Hart, Electric properties of tissues, in: Wiley Encyclopedia of Biomedical Engineering, John Wiley & Sons, New York, 2006, pp. 3578–3589.
[63] I. Lackovic, R. Magjarevic, D. Miklavcic, Three-dimensional finite-element analysis of joule heating in electrochemotherapy and in vivo gene electrotransfer, IEEE Trans. Dielect. Electr. Insul. 16 (2009) 1338–1347.
[64] S. Corovic, I. Lackovic, P. Sustaric, T. Sustar, T. Rodic, D. Miklavcic, Modeling of electric field distribution in tissues during electroporation, Biomed. Eng. Online 12 (2013) 16.